# Click Chemistry Plays a Dual Role in Biodegradable Polymer Design

*Jinshan Guo, Zhiwei Xie, Richard T. Tran, Denghui Xie, Dadi Jin, Xiaochun Bai, and Jian Yang**

The need for soft and elastic scaffold materials to resemble the elastic nature of soft tissues has recently driven the development of various biodegradable elastomeric polymers in tissue engineering and drug delivery.[1–10] As a substitute for the native extracellular matrix (ECM) of a target tissue or organ, the ideal scaffold material should be not only soft and elastic, but also amenable to surface biofunctionalization to mediate cell and tissue responses.[6,8,10–12] A number of biodegradable elastomeric polymers such as poly(glycerolsebacate) (PGS),[2,9] poly(ε-caprolactone) (PCL),[2,9] and citrate-based biodegradable elastomers (CABEs) such as poly (1,8-octanediol citrate) (POC),[1,4,7] crosslinked urethane-doped polyester elastomers (CUPE),[5] poly(alkylene maleate citrates) (PAMCs),[13] and biodegradable photoluminescent polymers (BPLPs)[6] have been synthesized to demonstrate their potential in tissue engineering. However, most of these materials are mechanically weak, with a tensile strength at dry state typically no more than 10 MPa,[1–4,7,9] which is significantly lower than that of human anterior cruciate ligaments (38 MPa). Unfortunately, these materials become even weaker when fabricated into porous scaffolds and/or used *in vivo* in physiological wet conditions significantly limiting their use in various tissue engineering applications.[3]

Effectively balancing the mechanical properties, biofunctionalizition, and biodegradation of the above polymers, especially site- or ligand-specific biofunctionalization to regulate cell/tissue-biomaterial interactions, has been a challenge.[14] In terms of addressing concerns on the weak mechanical strength of the existing elastomers, the introduction of urethane or amine groups into polyesters has been proved to be an effective way for improving mechanical strength of polyester elastomers.[2,5,6,9,15] Increasing the cross-linking density may serve as another strategy.[1,7] However, improving mechanical properties by increasing polymer cross-linking densities and introducing urethane/urea bonds in elastomers sacrifice the limited functional groups for future bioconjugation/functionalizion and also slow down the material degradation rate. As one of the most effective, site-specific reactions that are tolerant to water, oxygen, and a wide range of functionalities, azide-alkyne cycloaddition (AAC, click chemistry),[14,16–25] especially copper-free click chemistry, has been a promising method for functionalizing bio-related systems.[14,22,23] It was also reported that the triazole rings resulting from click chemistry could imitate amide bonds serving as mechanical strength improving moieties.[20,26] Herein, click chemistry was introduced into CABEs to serve a dual role and create a novel material chemistry design strategy to simultaneously improve the bulk material mechanical strength and enable easy surface site-specific biofunctionalization, which can also be broadly applied to other functional biodegradable polymer design.

By introducing azide and alkyne functional diols, azide (pre-POC-$N_3$) and alkyne (pre-POC-Al) functionalized POC prepolymers were synthesized (**Scheme 1**A). Without the use of any toxic copper-catalysts, pre-POC-$N_3$ and pre-POC-Al were mixed and crosslinked via a thermal synchronous binary (TSB) cross-linking mechanism. In the TSB cross-linking, thermal click reaction between azide and alkyne groups and esterification between –COOH and –OH groups[27,28] took place simultaneously to form TSB crosslinked POC-click elastomers (Scheme 1B). POC-click elastomers possessed much improved mechanical strength (up to 40 MPa of tensile stress). The uniquely introduced extra azide groups on POC-click polymers also enabled the easy conjugation of heat-labile biomolecule such as peptides or proteins via another copper-free click reaction, strain-promoted azide-alkyne cycloaddition (SPAAC) in aqueous environment at room temperature or 37 °C. Collagen mimetic peptide p15, which can effectively promote the adhesion and proliferation of endothelial cells (ECs),[12] was exemplarily clicked onto POC-click films and scaffolds (Scheme 1B and S1) through SPAAC.

Pre-POC-$N_3$ and pre-POC-Al were synthesized separately by polycondensation of citric acid (CA), 1, 8-octanediol (OD), and azide or alkyne functional diols (diazido-diol [DAzD] or alkyne-diol [AlD] as shown in Scheme 1A via a one-pot synthesis process.[1,4,7] The successful introduction of azide or alkyne groups into the pre-polymers was verified by FTIR and NMR (Figure S1 and S2), as indicated by the appearance of the characteristic infrared absorption peak of azide group (2100 $cm^{-1}$ in FTIR) or peak of the protons -C**H**$_2$-C≡CH in $^1$H-NMR (around 4.5 ppm),

Dr. J. Guo, Dr. Z. Xie, Dr. R. T. Tran, Prof. J. Yang
Department of Biomedical Engineering
Materials Research Institute
The Huck Institutes of The Life Sciences
The Pennsylvania State University
University Park, PA 16802, USA
E-mail: jxy30@psu.edu
D. Xie, D. Jin, X. Bai
Academy of Orthopedics of Guangdong Province
Guangzhou, 510630, China
Department of Orthopedics
The Third Affiliated Hospital
Southern Medical University
Guangzhou, 510630, China

**DOI: 10.1002/adma.201305162**

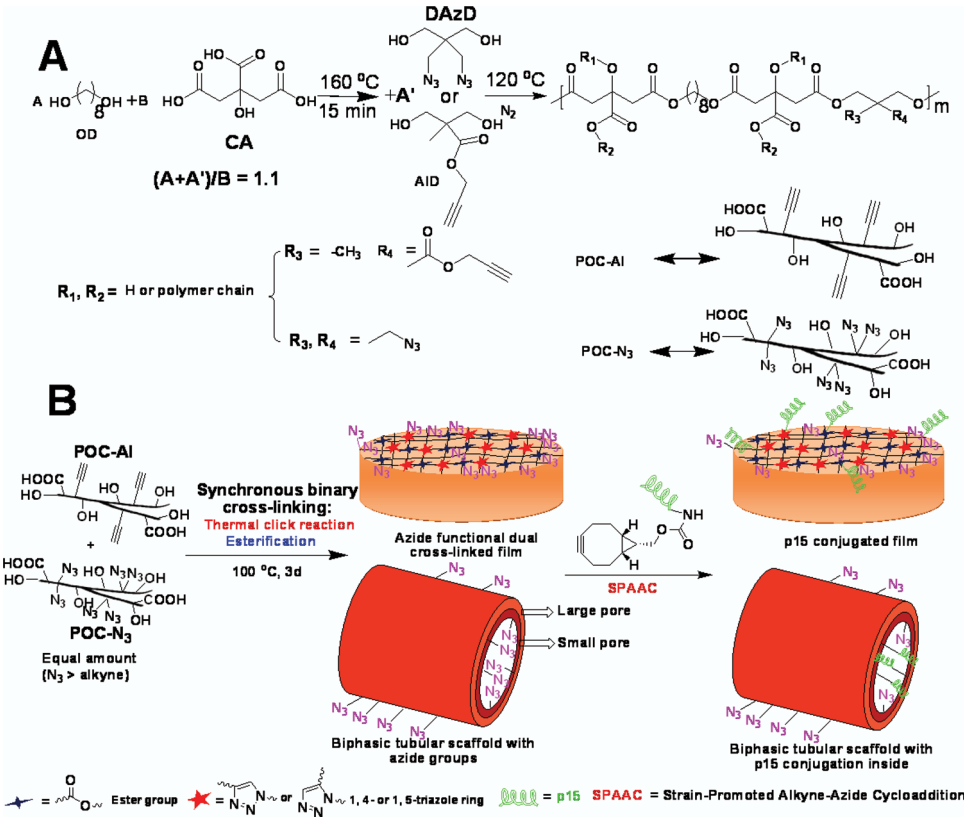


**Scheme 1.** (A) Synthesis of functional POC pre-polymers: POC-$N_3$ and POC-Al; (B) Synchronous binary cross-linked POC-click films, porous tubular biphasic scaffold preparation, and p15 conjugation by strain-promoted azide-alkyne cycloaddition (SPAAC).

respectively. The intensities of both peaks increased with an increase of feeding ratios of the functional diols to OD, indicating the increasing contents of azide or alkyne groups in the corresponding pre-POC-$N_3$-x or pre-POC-Al-x (x = 1, 2 or 3). Here, "x" represents the molar ratio of DAzD or AID to CA is x/10.

The optimized TSB cross-linking temperature of POC-click polymers was determined to be 100 °C (Figure S3), which is suitable for the thermal click reaction between azide and alkyne groups without affecting the reactivity of residual azide groups. The cross-linking density can be controlled by varying cross-linking times and the clickable pre-polymer ratios (pre-POC-$N_3$-x/pre-POC-Al-y, x, y = 1, 2 or 3). Some azide groups were preserved after cross-linking (Figure S4) since the specially chosen DAzD molecule contains two azide groups, while the AlD molecule contains only one alkyne group (Scheme 1A).

The mechanical properties of POC and POC-click polymers are shown in **Figure 1**A-H. The maximum tensile stress of both POC-click-x (POC-$N_3$-x, Al-x (w/w = 1/1)) and POC-$N_3$-x, Al-x (1/2) (x = 1, 2 or 3) polymer films are 10–40 MPa higher than that of POC (5 MPa), and 10–20 MPa higher than that of the corresponding POC-$N_3$-x and POC-Al-x films (Figure 1A and Table S1). These results suggested that although the replacement of relatively long-chain OD by short-chain DAzD or AlD diol monomers (Scheme 1) increases the tensile stress, undoubtedly, the introduction of thermal click reaction plays a predominant role. A more significant increase could be seen in the case of Young's modulus (Figure 1B), which relates directly to the cross-linking density (Table S1) of the film. The Young's modulus of POC-clik-3 and POC-$N_3$–3, Al-3 (1/2) films were as high as 300 MPa, which is nearly 60 times higher than that of POC (Table S1). The difference in the tensile stress or Young's modulus between POC-click-x and POC-$N_3$-x, Al-x (1/2) was insignificant due to the steric hindrance limiting the further progression of thermal click reaction. A similar phenomena could also be seen in the cases of POC-click polymers made from mixtures of POC-$N_3$-x and POC-Al-y (x, y = 1, 2 or 3 and x ≠ y) with different weight ratios (Figure S5). The elongation at break of the films showed an overall inverse correlation to cross-linking density, and displayed values all around 200–300% except for POC-click-3 and POC-$N_3$–3, Al-3 (1/2), which were all lower than 100% (Figure 1C and Table S1). POC-click-1 and POC-click-2 all showed elastomeric properties similar to POC (Figure 1D). Although the stress-strain curve of POC-click-3 had a yield point (Figure 1D) that is characteristic of plastic polymers, the same polymer became elastic after being immersed in PBS for about 24 hrs (Figure 1E), indicating that POC-click-3 can still serve as an elastomeric material *in vivo* (wet conditions). POC-click wet mechanical strengths were stronger than that of another citrate-based mechanically strong elastomer, CUPE.[5] When the cross-linking time was increased from 0.5 day to 3 days, the tensile stress and Young's modulus of POC-click polymers showed a remarkable and continuous increase, especially for POC-click-1 and POC-click-2, while POC only showed very limited improvement during the same time

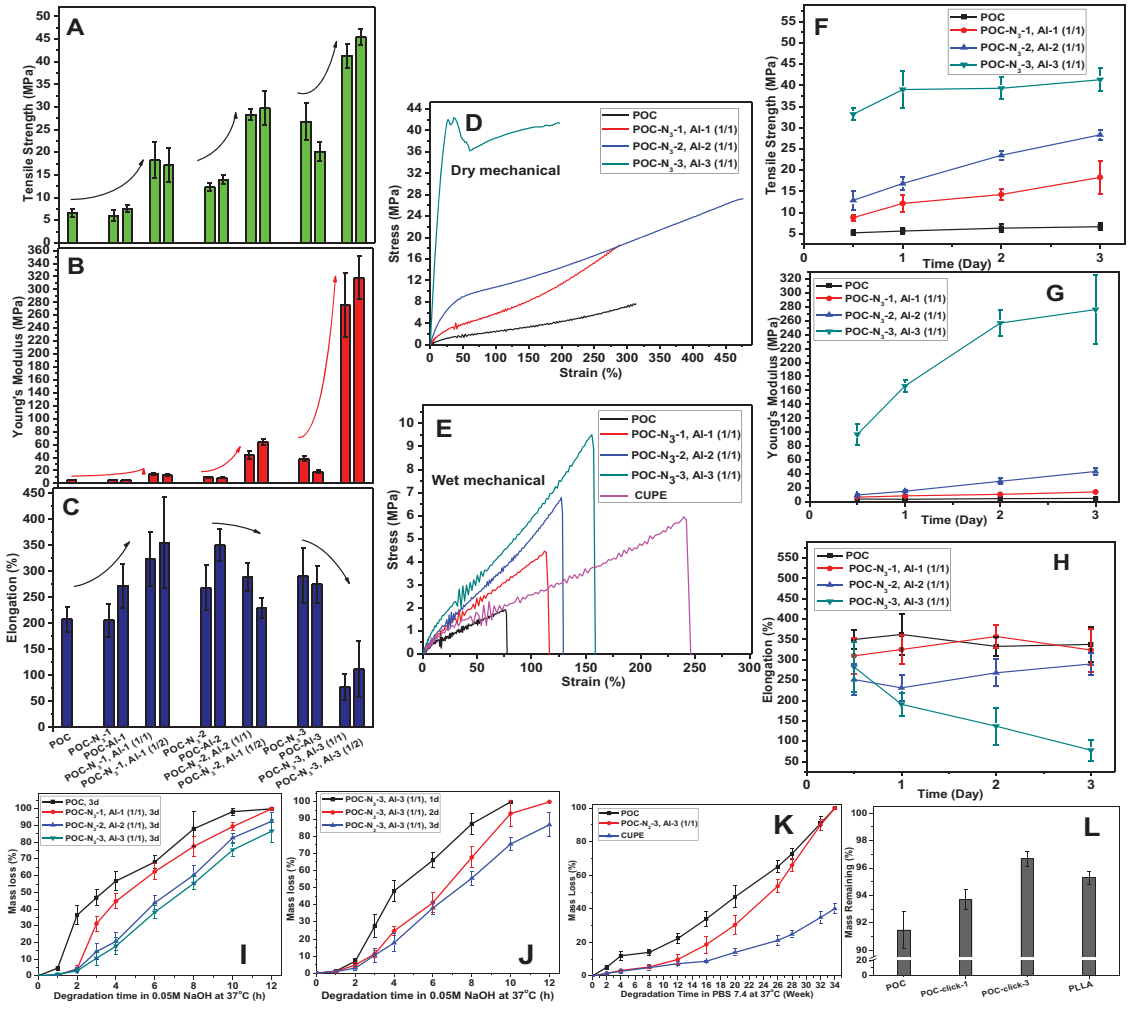


**Figure 1.** Mechanical properties of polymer films: Tensile strength (**A**), Young's modulus (**B**) and Elongation at break (**C**) of cross-linked films (all 100 °C, 3d) of POC, POC-$N_3$ series, POC-Al series, and TSB cross-linked POC-click series (1/1 and 1/2 between the parentheses represents the weight ratio between pre-POC-$N_3$-x and pre-POC-Al-x, x = 1, 2, or 3). (**D**) Tensile stress-strain curves of POC-click series and POC cross-linked films (100 °C, 3d) under dry condition. (**E**) Wet mechanical properties: Tensile stress-strain curves of POC-click series, POC and CUPE cross-linked films (100 °C, 3d) after being immersed in PBS (pH 7.4) for around 24 hrs. (**F**, **G** and **H**). The change of mechanical properties of POC-click and POC films after heating at 100 °C for different times: Tensile strength (**F**), Young's modulus (**G**) and Elongation at break (**H**). Degradation study of POC-click polymer series and controls (POC or/and CUPE/PLLA) *in vitro*, in 0.05M NaOH solution (**I**, **J**), PBS (pH 7.4) (**K**), and 20 weeks *in vivo* (**L**). All the polymer films used were cross-linked at 100 °C for 3 days except where specified otherwise. Films with thicknesses of 0.15–0.30 mm and 0.75–0.95 mm were used in *in vitro* degradations in 0.05M NaOH or PBS solutions (**I**, **j** and **K**) and in vivo (**L**) degradation, separately.

period (Figure 1F and 1G). These results further demonstrate the impact of thermal click reactions on mechanical properties. The elongation of the polymer films showed no significant change when the cross-linking time increased (Figure 1H), except in the case of POC-click-3. The above investigations suggested that the introduction of click chemistry into POC could significantly improve the mechanical strengths of the TSB crosslinked polymers. To further expand click chemistry-based elastomers, clickable biodegradable photoluminescent polymer (BPLP-Ser)[6] and urethane-doped polyester (UPE)[5] were also synthesized. The TSB crosslinked polymers (CBPLP-Ser-click, CUPE-click) also showed significantly enhanced mechanical strengths compared to normal BPLP and CUPE (Figure S6).

The *in vitro* and *in vivo* degradation results of different polymers are shown in Figure 1E-H. POC-click polymers degraded slower than POC in 0.05M NaOH solution. POC-click-1 and POC degraded completely, but around 80% of POC-click-3 degraded after 12 hrs incubation. The degradation rates decreased when the cross-link density increased (Figure 1I). A similar trend was found with an increase of cross-linking times from 1 day to 3 days (Figure 1J). The degradation profiles of POC-click-3, POC, and CUPE in PBS (pH 7.4) are shown in Figure 1K. During the first 12 weeks, POC-click-3 demonstrated a mass loss of no more than 5% while POC lost around 25% of its initial mass. After the 12$^{th}$ week, however, POC-click-3 entered into a relatively rapid degradation period and the mass loss eventually caught up with that of POC by the 32$^{nd}$ week. POC-click-3 and POC were completely degraded after 34 weeks, while no more than 40% of CUPE was degraded. The "first slow then fast" degradation phenomenon of

POC-click-3 was considered to be related to its chemical structure (Scheme S1). Both ester bonds (green) and triazole rings (red) exist in POC-click-3. Ester bonds degraded much faster than triazole rings,[29] which is why initially more hydrophobic POC-click-3 degraded much slower than relatively hydrophilic pure polyester, POC. Once the ester bonds surrounding DAzD (in the blue circle in Scheme S2) in POC-click-3 were hydrolyzed, the DAzD crosslink points were destroyed. Along with the destruction of the DAzD cross-link points, the degradation rate of POC-click-3 became even faster than that of POC, which allowed the mass loss to catch up with that of POC. The "first slow then fast" degradation characteristic of POC-click polymers is favorable in many biomedical applications especially tissue engineering, as the preservation of mechanical strength in the initial period after implantation before tissue regeneration is preferred. After 20 weeks of subcutaneous implantation in the back of Sprague Dawley (SD) rats, the mass loss of POC-click-1, POC-click-3, POC, and PLLA were 6.28%, 3.28%, 9.54% and 5.71% respectively (Figure 1L). On another note, we have previously demonstrated that partially replacing 1, 8-octanediol with N-methyldiethanolamine (MDEA) in POC synthesis could simultaneously improve the polymer mechanical strength and degradation rate.[7] This MDEA strategy may also be applied to POC-click synthesis to further increase the material mechanical strength and degradation rate.

The residual azide groups on POC-click polymers (Figure S4) have paved the way for convenient bioactive molecule conjugation on the surface of POC-click films or scaffolds via SPAAC (Scheme 1B). As an example, collagen mimetic peptide p15, which can effectively promote the adhesion and proliferation of ECs, was conjugated onto the surface of POC-click-3 films by SPAAC (Scheme 1B and S1), and the viability/proliferation of human umbilical vein endothelial cells (HUVEC) on POC-click-3-p15 films were investigated. The successful conjugation of p15 onto the surface of POC-click-3 films was confirmed by the decrease of azide absorption peak (2100 $cm^{-1}$) after p15 conjugation shown in the FTIR spectra (Figure S7A) as well as the appearance of the characteristic peak of guanidine groups on p-15 peptides as shown in the UV-vis spectra (Figure S7B) after Sakaguchi reactions (Figure S8).[11] The effect of p15 conjugation on HUVEC proliferation was investigated by MTT assay, Live/Dead assay, and SEM using untreated POC-click-3 films as control (Figure S7C and 2A). From the MTT results (Figure S7C), it could be seen that the initial HUVEC cell number (day 1) on POC-click-3-p15 films was higher than that of untreated POC-click-3 films. However, the difference between them was not significant, which could also be seen from the Live/Dead assay images (**Figure 2**A). After the initial cell adhesion, HUVEC proliferation on POC-click-3-p15 films was obviously faster than that on untreated POC-click-3 films, similar to the trend on p15-modified PTFE as reported previously.[11] The HUVEC cell density on POC-click-3-p15 films at day 7 nearly doubled compared to the control POC-click-3 films. The Live/Dead images also supported the same growth pattern. Both Live/Dead assay images and SEM images (Figure 2A) showed the characteristic cobblestone morphology of live cells (green fluorescence in Live/Dead images). Only few red fluorescence (dead cells) positive cells were found in Live/Dead images. The number of dead HUVEC cells on POC-click-3-p15 films was much less than that on POC-click-3 films (Figure 2A). The HUVEC cell proliferation results show that the p15 conjugation on POC-click-3 surfaces could promote HUVEC cell adhesion and proliferation. Using the convenient SPAAC method, other bioactive molecules can also be easily conjugated onto POC-click films or scaffolds in an amiable condition with much less risk of destroying the bioactivities of the conjugated bioactive molecules.

To further support the potentials of POC-click polymers in tissue engineering applications, especially blood vessel tissue engineering, POC-click-3 was chosen as a representative material to be molded into anatomically correct tubular biphasic scaffolds (TBS), which consist of an inner thin porous phase (pore size of 1–20 μm) to simulate the native elastic lamina and outer macroporous phase (pore size of 150–250 μm). The mechanical properties of POC-click-3 scaffolds were tested and compared with TBSs made by POC and CUPE. Furthermore, the conjugation of p15 onto the inner surface of POC-click TBS was also conducted. It was demonstrated that a rough inner lumen surface is more favorable for the growth of ECs, and pore size of 1–20 μm is preferable for the compartmentalization of ECs and smooth muscle cells (SMCs) simulating the elastic lamina in native vessels. Pore sizes of 150–250 μm have been proven to be ideal for the growth of fibroblasts and SMCs and the formation of extracellular matrix (ECM).[3,30] The photographs and representative SEM images of POC-click TBS shown in Figure 2B clearly imply the soft nature of the biphasic scaffold. Although molded into a porous scaffold, the tensile strength and Young's modulus of POC-click TBS (around 5 and 17 MPa, respectively) are all much higher than that of POC TBS (~1 and 1.2 MPa respectively), and even higher than that of CUPE TBS (~3.8 and 4 MPa, respectively) (Figure 2C). The tensile strength of native radial arteries is 2.68 ± 1.81 MPa. Although the elongation of POC-click TBS is somewhat lower than that of CUPE TBS, it is higher than that of POC TBS (Figure 2D). Burst pressure is another key parameter that determines the suitability of a vascular scaffold for implantation. As seen from Figure 2E, the burst pressure of POC-click TBS is around 5000 mmHg, which is higher than that of POC (below 1000 mmHg) and CUPE (around 3500 mmHg) TBSs, and also higher than that of both saphenous veins and mammary arteries (1599 ± 877 and 4225 ± 1368 mmHg, respectively), which are currently used as the "gold standards" of vascular grafts.[31] The suture retention strength of POC-click-3 TBS is around 3.75 N, which is higher than both POC TBS (~0.75 N) and CUPE TBS (~3.0 N) (Figure 2F) and also significantly higher than the reported value of 1.20 ± 0.23 N required for suturing arterial vascular grafts.[3] The above results provide evidence that POC-click TBS possess sufficient mechanical strengths to serve as off-the-shelf vascular grafts. In addition to the superior mechanical properties of POC-click vascular grafts compared with POC and even CUPE grafts, the residual azide groups on the surface of POC-click scaffolds enabled an easy bioactive molecules conjugation through SPAAC. P15 could be easily conjugated onto the surface of the inner layer of POC-click TBS, which was confirmed by FTIR spectra (Figure S9A) and UV-vis spectra (Figure S9B) as previously described.

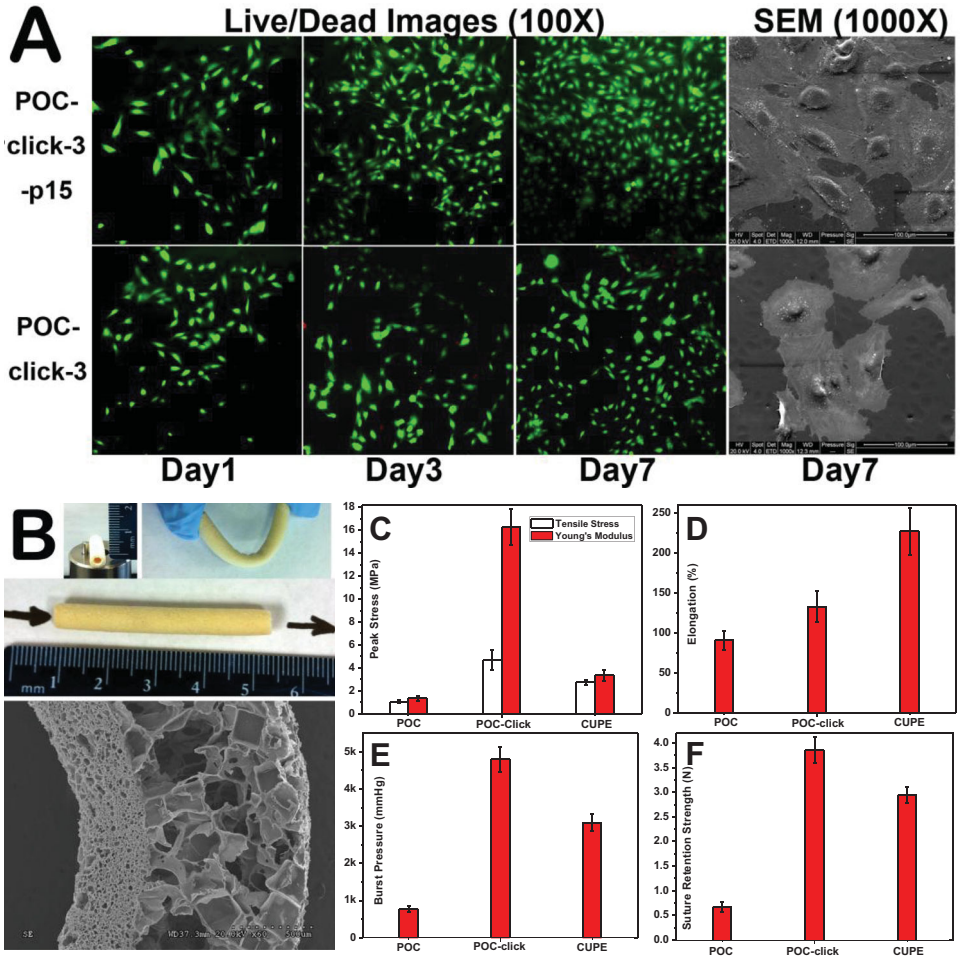


**Figure 2.** **A**: Live/Dead assay (1, 3, and 7 days) and SEM (7 day) images of HUVECs proliferation on POC-click-3-p15 films and POC-click-3 films; **B**: Photographs and representative SEM image of POC-click-3 tubular porous biphasic scaffold. The mechanical properties of POC, POC-click (using POC-click-3), and CUPE tubular biphasic scaffold (TBS): tensile strength and Young's modulus (**C**) and elongation at break (**D**) in uniaxial tension experiments; vascular graft burst pressure results (**E**) and graft suture retention strengths (**F**).

In conclusion, the introduction of click chemistry into citrate-based biodegradable elastomer (CABE), such as poly (1, 8-octanediol citrate) (POC), can vastly increase the mechanical strength of the resulting polymer and greatly facilitate biomolecule conjugation through the clickable moieties. POC-click elastomers were polymerized under a unique thermal synchronous binary (TSB) cross-linking mechanism (post-esterification between –COOH and –OH groups and thermal click reactions between newly introduced alkyne and azide groups). Furthermore, the residual azide groups on the surface of POC-click films and scaffolds enabled facile and efficient surface conjugation of bioactive molecules through strain-promoted azide-alkyne cycloaddition (SPAAC). The present work successfully combined two kinds of copper-free click reactions, thermal click reaction and SPAAC, which serve as a novel cross-linking method and efficient surface conjugation route, respectively. A dual role application of click chemistry can also be extended to the other CABEs such as PAMC, CUPE and BPLP and possibly many other biodegradable polymers such as PGS and PCL. We believe that the clickable biodegradable elastomer design will greatly expand the application of biodegradable polymers, especially for CABEs in many biomedical areas such as tissue engineering, drug delivery, orthopedic fixation devices, and other medical implants where mechanical properties and biofunctionality are key in their success. The synthesis of clickable POC represents an innovation in the design of functional biodegradable polymers and may facilitate their translation in diversified biomedical applications.

## Supporting Information

Supporting Information is available from the Wiley Online Library or from the author.

## Acknowledgements

This work was supported in part by a National Institute of Biomedical Imaging and Bioengineering (NIBIB) Award EB012575, a National Cancer Institute (NCI) Award CQ182670, National Science Fundation

(NSF) Awards (DMR1313553, CMMI 1266116), and a National Natural Sciences Foundation of China Award (31228007).

Received: October 16, 2013
Revised: November 15, 2013
Published online: December 23, 2013

[1] J. Yang, A. R. Webb, G. A. Ameer, *Adv. Mater.* **2004**, *16*, 511.
[2] W. Wu, R. A. Allen, Y. Wang, *Nat Med* **2012**, *18*, 1148.
[3] J. Dey, H. Xu, K. T. Nguyen, J. Yang, *J. Biomed. Mater. Res. A* **2010**, *95A*, 361.
[4] J. Yang, D. Motlagh, J. B. Allen, A. R. Webb, M. R. Kibbe, O. Aalami, M. Kapadia, T. J. Carroll, G. A. Ameer, *Adv. Mater.* **2006**, *18*, 1493.
[5] J. Dey, H. Xu, J. Shen, P. Thevenot, S. R. Gondi, K. T. Nguyen, B. S. Sumerlin, L. Tang, J. Yang, *Biomaterials* **2008**, *29*, 4637.
[6] J. Yang, Y. Zhang, S. Gautam, L. Liu, J. Dey, W. Chen, R. P. Mason, C. A. Serrano, K. A. Schug, L. Tang, *Proc. Natl. Acad. Sci. USA* **2009**, *106*, 10086.
[7] J. Yang, A. R. Webb, S. J. Pickerill, G. Hageman, G. A. Ameer, *Biomaterials* **2006**, *27*, 1889.
[8] M. Mehdizadeh, H. Weng, D. Gyawali, L. Tang, J. Yang, *Biomaterials* **2012**, *33*, 7972.
[9] M. C. Serrano, E. J. Chung, G. A. Ameer, *Adv. Funct. Mater.* **2010**, *20*, 192.
[10] A. de Mel, G. Jell, M. M. Stevens, A. M. Seifalian, *Biomacromolecules* **2008**, *9*, 2969.
[11] Z. Zhang, Y. Lai, L. Yu, J. Ding, *Biomaterials* **2010**, *31*, 7873.
[12] C. Li, A. Hill, M. Imran, *J. Biomater. Sci. Polym. Ed.* **2005**, *16*, 875.
[13] R. T. Tran, P. Thevenot, D. Gyawali, J.-C. Chiao, L. Tang, J. Yang, *Soft Matter* **2010**, *6*, 2449.
[14] S. F. M. van Dongen, P. Maiuri, E. Marie, C. Tribet, M. Piel, *Adv. Mater.* **2013**, *25*, 1687.
[15] H. Cheng, P. S. Hill, D. J. Siegwart, N. Vacanti, A. K. R. Lytton-Jean, S.-W. Cho, A. Ye, R. Langer, D. G. Anderson, *Adv. Mater.* **2011**, *23*, H95.
[16] D. Zhao, S. Tan, D. Yuan, W. Lu, Y. H. Rezenom, H. Jiang, L.-Q. Wang, H.-C. Zhou, *Adv. Mater.* **2011**, *23*, 90.
[17] C. He, X. Zhuang, Z. Tang, H. Tian, X. Chen, *Adv. Healthcare Mater.* **2012**, *1*, 48.
[18] H. Tian, Z. Tang, X. Zhuang, X. Chen, X. Jing, *Prog. Polym. Sci.* **2012**, *37*, 237.
[19] J. Guo, F. Meng, X. Jing, Y. Huang, *Adv. Healthcare Mater.* **2013**, *2*, 784.
[20] J. Guo, Y. Wei, D. Zhou, P. Cai, X. Jing, X.-S. Chen, Y. Huang, *Biomacromolecules* **2011**, *12*, 737.
[21] K. Liang, G. K. Such, Z. Zhu, Y. Yan, H. Lomas, F. Caruso, *Adv. Mater.* **2011**, *23*, H273.
[22] C. R. Becer, R. Hoogenboom, U. S. Schubert, *Angew. Chem. Int. Ed. Engl.* **2009**, *48*, 4900.
[23] R. Manova, T. A. van Beek, H. Zuilhof, *Angew. Chem. Int. Ed. Engl.* **2011**, *50*, 5428.
[24] D. A. Heller, Y. Levi, J. M. Pelet, J. C. Doloff, J. Wallas, G. W. Pratt, S. Jiang, G. Sahay, A. Schroeder, J. E. Schroeder, Y. Chyan, C. Zurenko, W. Querbes, M. Manzano, D. S. Kohane, R. Langer, D. G. Anderson, *Adv. Mater.* **2013**, *25*, 1449.
[25] T. Gong, B. J. Adzima, N. H. Baker, C. N. Bowman, *Adv. Mater.* **2013**, *25*, 2024.
[26] W. S. Horne, M. K. Yadav, C. D. Stout, M. R. Ghadiri, *J. Am. Chem. Soc.* **2004**, *126*, 15366.
[27] J. Guo, F. Meng, X. Li, M. Wang, Y. Wu, X. Jing, Y. Huang, *Macromol. Biosci.* **2012**, *12*, 533.
[28] J. Hong, Q. Luo, X. Wan, Z. S. Petrovi , B. K. Shah, *Biomacromolecules* **2011**, *13*, 261.
[29] K. Yao, J. Wang, W. Zhang, J. S. Lee, C. Wang, F. Chu, X. He, C. Tang, *Biomacromolecules* **2011**, *12*, 2171.
[30] Y. Zhang, R. T. Tran, I. S. Qattan, Y.-T. Tsai, L. Tang, C. Liu, J. Yang, *Biomaterials* **2013**, *34*, 4048.
[31] N. L'Heureux, N. Dusserre, G. Konig, B. Victor, P. Keire, T. N. Wight, N. A. F. Chronos, A. E. Kyles, C. R. Gregory, G. Hoyt, R. C. Robbins, T. N. McAllister, *Nat. Med.* **2006**, *12*, 361.

ADVANCED MATERIALS

# Supporting Information

for *Adv. Mater.*, DOI: 10.1002/adma.201305162

# Click Chemistry Plays a Dual Role in Biodegradable Polymer Design

*Jinshan Guo, Zhiwei Xie, Richard T. Tran, Denghui Xie, Dadi Jin, Xiaochun Bai, and Jian Yang**

# Supporting Information

for *Adv. Mater.*, DOI: 10.1002/adma.201305162

**Click chemistry plays a dual role in biodegradable polymer design**

*Jinshan Guo, Zhiwei Xie, Richard T. Tran, Denghui Xie, Dadi Jin, Xiaochun Bai, and Jian Yang**

Dr. J. Guo, Dr. Z. Xie, Dr. R. T. Tran, Prof. J. Yang
Department of Biomedical Engineering, Materials Research Institute, The Huck Institutes of The Life Sciences, The Pennsylvania State University, University Park, PA 16802, USA

D. Xie, D. Jin, X. Bai
Academy of Orthopedics of Guangdong Province, Guangzhou, 510630, China; Department of Orthopedics, The Third Affiliated Hospital, Southern Medical University, Guangzhou, 510630, China

*Corresponding author: Jian Yang, e-mail: jxy30@psu.edu
W340 Millennium Science Complex, The Pennsylvania State University, University Park, PA 16802. Tel.: (+1) 814-865-1278;

## Experimental Section

### Materials

2, 2-Bis(azidomethyl)propane-1,3-diol (diazido-diol monomer, DAzD) was synthesized as described elsewhere. [1, 2] Propargyl 2, 2-bis(hydroxyl-methyl)propionate (alkyne-diol monomer, AlD) was also synthesized according to previous literatures. [3, 4] The p15 peptide ($NH_2$-Gly-Thr-Pro-Gly-Pro-Gln-Gly-Ile-Ala-Gly-Gln-Arg-Gly-Val-Val-$CONH_2$) was purchased from United Peptide Corp.

(Rockville, MD). Click-easy ™ BCN N-hydroxysuccinimide ester I (used for Strain-promoted alkykyne-azide cycloaddition (SPAAC)) was purchased from Berry & Associates Inc. All other reagents were purchased from Sigma-Aldrich and used without further purification.

**General Measurements**

$^1$H-NMR spectra of pre-polymers were recorded on a JNM ECS 300 spectrometer (JEOL, Tokyo, Japan) in DMSO-$d_6$. Attenuated total reflection Fourier transform infrared (ATR-FTIR) spectra were measured with a Nicolet 6700 FTIR spectrometer using cast films of pre-polymer in 1, 4-dioxane or cross-linked polymer films directly. The morphology of tubular scaffolds was observed by scanning electron microscope (SEM) (Hitachi 3500 N, EPIC). UV-vis spectra were recorded using UV-2450 spectrometer (Shimadzu, Japan) with a minimum wavelength resolution of 0.2 nm.

**Polymer Syntheses and Film Preparation**

**POC Synthesis**

Poly (1, 8-octanediol-*co*-citrate) (POC) was synthesized according to previous work. [5, 6] Briefly, a mixture of citric acid (CA) and 1,8-octanediol (OD) (molar ratio of CA: OD was 1: 1.1) was melted at 160$^o$C for about 20 min. The temperature was reduced to 140$^o$C and the reaction was continued for another ~45 min until the stir bar was twitched at 60 rpm. The crude product was purified by precipitating the oligomer/1,4-dioxane solution in water followed by freeze-drying. $^1$H NMR (300 MHz; DMSO-*d*6; δ, ppm) of pre-POC: 1.15 (s, -$OCH_2CH_2(C\mathbf{H}_2)_4$- from OD), 1.50 (s, -$OCH_2C\mathbf{H}_2$-), 2.50-2.90 (m, -OCO-$C\mathbf{H}_2$-C(OH)(COO-)- from CA), 3.60 (br,

-C**H**$_2$-OH from OD), 3.90-4.05 (br, -COOC**H**$_2$- from OD). FTIR of pre-POC (thin film, cm$^{-1}$): 1733 (COOR).

The POC pre-polymer was post-polymerized by heating in an oven at 100$^o$C for 3 days to create POC film. In this process, part of the un-reacted -COOH and -OH groups of pre-POC were cross-linked. In addition, POC samples with cross-linking times of 1 or 2 days were also prepared keeping the temperature unchanged. FTIR of POC film (cm$^{-1}$): 1735 (COOR).

**POC-click Synthesis**

Functional POC pre-polymers with azide (pre-POC-$N_3$) or alkyne (pre-POC-Al) groups were synthesized separately by the copolymerization of CA, OD, and azide or alkyne functional diols (DAzD or AlD in Scheme 1). After melting of the mixture of CA and OD at 160$^o$C, the reaction temperature was reduced to 120$^o$C followed by the addition of functional monomer (DAzD or AlD). The reaction was continued at 120$^o$C under nitrogen using a vent plug until the stir bar twitched at 60 rpm in which the reactions often took more than 2 hours. The purification processes was the same as that of POC pre-polymer. For pre-POC-$N_3$ series, the molar ratios of CA: OD: DAzD for pre-POC-$N_3$-1, pre-POC-$N_3$-2 and pre-POC-$N_3$-3 are 1: 1: 0.1, 1: 0.9: 0.2 and 1: 0.8: 0.3, respectively. $^1$H NMR (300 MHz; DMSO-*d6*; δ, ppm) of pre-POC-$N_3$: 1.15 (s, -OCH$_2$CH$_2$(C**H**$_2$)$_4$- from OD), 1.50 (s, -OCH$_2$C**H**$_2$-), 2.60-2.90 (m, -OCO-C**H**$_2$-C(OH) (COO-)- from CA), 3.20-3.50 (br, -C**H**$_2$-$N_3$ from DAzD, -C**H**$_2$-OH from OD and DAzD), 3.80-4.05 (br, -COOC**H**$_2$- from OD and DAzD). FTIR of pre-POC-$N_3$ (thin film, cm$^{-1}$): 2109 (-$N_3$, strong), 1735 (COOR). Similarly,

for pre-POC-Al series, the monomers ratios of CA: OD: AlD for pre-POC-Al-1, pre-POC-Al-2 and pre-POC-Al-3 are also 1: 1: 0.1, 1: 0.9: 0.2 and 1: 0.8: 0.3, respectively. $^{1}$H NMR (300 MHz; DMSO-*d*6; δ, ppm) of pre-POC-Al: 1.05 (s, C**H**$_3$- from AlD), 1.20 (s, -OCH$_2$CH$_2$(C**H**$_2$)$_4$- from OD), 1.55 (s, -OCH$_2$C**H**$_2$- from OD), 2.60-2.90 (m, -OCO-C**H**$_2$-C(OH)(COO-)- from CA), 3.20-3.65 (br, -C**H**$_2$-OH from OD and AlD, -C≡C**H** from AlD), 3.85-4.15 (br, -COOC**H**$_2$- from OD and AlD), 4.60-4.70 (br, -C**H**$_2$-C≡CH from AlD). FTIR of pre-POC-Al (thin film, cm$^{-1}$): 2130 (-C≡CH, weak), 1735 (COOR). For clickable pre-polymer syntheses, one azide group-containing diols such as 2-(azidomethyl)-2-methylpropane-1,3-diol and two alkyne groups-containing diols such as 2,2-di(prop-2-ynyl)-propane-1,3-diol may also be used to react with CA and OD.

Although copper-catalyst alkyne-azide cycloaddition (CuAAC) may not always lead to high Cu content in final polymers, –COOH groups in citrate-based polymer may chelate Cu ions, which makes purification problematic. It is also considered favorable to synthesize biomaterials without using any potentially toxic metal ions. Herein, thermal synchronous binary (TSB) cross-linked POC films (POC-Click) were formed by heating the mixture of pre-POC-N$_3$ and pre-POC-Al at 100$^{o}$C for 3 days. In the process, post-esterification between un-reacted –COOH and –OH groups of both pre-polymers as well as thermal alkyne-azide cycloaddition (AAC, also named thermal click reaction) between alkyne groups of pre-POC-Al and azide groups of pre-POC-N$_3$ took place in the same post-polymerization process leading to the name thermal synchronous binary (TSB) cross-linked POC, or POC-click for convenience.

POC-click samples with different cross-linking densities were fabricated by adjusting the weight ratios between pre-POC-$N_3$ and pre-POC-Al (from 1/1 to 1/2, 1/4, even 1/6), the functional group contents in pre-POC-$N_3$ (from pre-POC-$N_3$-1, pre-POC-$N_3$-2 to pre-POC-$N_3$-3) and pre-POC-Al (from pre-POC-Al-1, pre-POC-Al-2 to pre-POC-Al-3), and the heating times (from 1, 2 to 3 days), which are shown in Figure 1, 2, S5 and Table S1. FTIR of POC-click film ($cm^{-1}$): 2109 (-$N_3$, still have), 1736 (COOR).

**TSB crosslinking of POC-click polymers**

To obtain optimized TSB cross-linking conditions of POC-click polymers, especially for thermal click reaction, the thermal stability of azide group were first investigated by heating sole pre-POC-$N_3$-1 (the molar ratio of CA: OD: DAzD is 1: 1: 0.1) at 80, 100 or 120$^o$C for different periods. The FTIR spectra of the obtained polymer films are shown in Figure S3A. It can be seen that the characteristic infrared absorption peak of azide group at 2100 $cm^{-1}$remained unchanged after heating at 80 or 100$^o$C for 1, 2 or even 3 days, but diminished after heating at 120$^o$C for 3 days. The above results suggested that azide groups were stable and can maintain their reactivity at 80 and 100$^o$C for at least 3 days, but became unstable when the temperature increased to 120$^o$C for longer heating times (3 days). The POC-$N_3$ synthesis was conducted at 120$^o$C as the reaction only lasted for about 3 hours. Furthermore, equal-weight of pre-POC-$N_3$-1 and pre-POC-Al-1 were mixed together and heated at either 80 or 100$^o$C for different times. As shown in Figure S3B, the intensity of the azide absorption peak in FTIR spectrums of POC-$N_3$-1, Al-1 films at 2100 $cm^{-1}$

remained unchanged after heating at 80$^{o}$C for up to 4 days, but decreased quickly after heating at 100$^{o}$C for 1, 2, or 3 days, suggesting that 100$^{o}$C is suitable for thermal click reaction. From the above investigation, the optimized TSB crosslinking temperature was determined to be 100$^{o}$C.

**CUPE and CUPE-click**

Crosslinked urethane-doped polyester pre-polymer (UPE) was synthesized as described previously using 1, 6-hexamethyl diisocynate (HDI) as a chain-extender. [7] The weight ratio between pre-POC and HDI was 1: 0.22. Similarly, UPE-$N_3$ and UPE-Al were also synthesized using POC-$N_3$-1 and POC-Al-1 pre-polymers, respectively, to replace POC pre-polymer. The weight ratio between the pre-polymer and HDI was kept the same as that of UPE. CUPE films were prepared by heating UPE at 100$^{o}$C for 3 days. Similarly, CUPE-$N_3$, CUPE-Al and CUPE-click (thermal cured film of equal-weight mixture of UPE-$N_3$ and UPE-Al) films were also formed under the same condition.

**cBPLP-Ser and cBPLP-Ser-click**

BPLP-Ser (biodegradable photoluminescent polymers reacted with L-Ser) was synthesized as described previously using CA, OD and L-Ser with a ratio of 1.0: 1.1: 0.2, respectively. [8] Similarly, BPLP-Ser-$N_3$ and BPLP-Ser-Al were also synthesized using CA, OD, DAzD or AlD ($N_3$ or alkyne functional monomer) and L-Ser with the molar ratio of 1.0: 1.0: 0.1: 0.2, respectively. Cross-linked BPLP-Ser (cBPLP-Ser) films were formed by heating BPLP-ser at 100$^{o}$C for 3 days. Also, cBPLP-Ser-$N_3$, cBPLP-Ser-Al as well as cBPLP-Ser-N3, Al (equal-weight mixture of BPLP-Ser-$N_3$

and BPLP-Ser-Al) films were prepared by cross-linking corresponding polymers under the same condition as cBPLP-Ser.

**Polymer Characterization**

The thermal properties of cross-linked polymers were characterized by differential scanning calorimetry (DSC, -50$^{o}$C~150$^{o}$C) and thermal gravimetric analysis (TGA, 20$^{o}$C~800$^{o}$C) at a heating rate of 10°C/min under nitrogen atmosphere. The glass transition temperature ($T_g$) was determined by the first heating run to avoid the effect of further cross-linking in the measurement process. The decomposition temperature ($T_d$) was defined as the temperature with 5% weight loss of the samples.

The water-in-air contact angles of POC, POC-click-1 [POC-$N_3$-1, Al-1 (1/1)], POC-click-2 [POC-$N_3$-2, Al-2 (1/1)], POC-click-3 [POC-$N_3$-3, Al-3 (1/1)], and PLLA films were measured at room temperature using the sessile drop method [10] by a Rame-Hart goniometer and imaging system (Rame-Hart Inc., Mouttain Lake, NJ) within 10 s after dropping. Four independent measurements at different sites were averaged. The change of water-in-air contact angle with time was also monitored from 0 to 30 minutes after water was dropped on the surface of the films. The results are shown in Figure S10.

Elastomer densities were measured by a Mettler Toledo (Greifense, Switzerland) balance with a density determination kit based on Archimedes' principle with distilled water as the auxiliary liquid.

Mechanical tests were conducted with an MTS Insight 2 machine fitted with a 500 N load cell. The samples were cut into a rectangle shaped specimens and elongated to

failure. The Young's modulus was calculated by measuring the gradient from 0 to 10% of elongation of the stress-strain curve. Eight specimens per sample were tested and averaged.

The cross-linking density and molecular weight between cross-linking sites were evaluated according to the theory of rubber elasticity using Eq. (1). [9]

$$n = \frac{E_0}{3RT} = \frac{\rho}{M_c} \quad (1)$$

Where $n$ represents the number of active network chain segments per unit volume (mol/m$^3$); $M_c$ represents the molecular weight between cross-linking sites (g/mol); $E_0$ represents Young's modulus (Pa); $R$ is the universal gas constant (8.3144 J/mol K); $T$ is the absolute temperature (K); and $\rho$ is the elastomer density (g/m$^3$) as measured via the method mentioned above.

Wet mechanical properties of the films were measured after immersing the films in PBS (pH 7.4) for 24 hrs until the hydrated weight of the films no longer increased.

***In Vitro* and *In Vivo* Degradation**

For *in vitro* degradation, disk–shaped specimens (7 mm in diameter, with thickness around 0.15-0.30 mm) were placed in tubes containing 10 mL of phosphate buffered saline (PBS, pH 7.4) or NaOH solution (0.05 M) and incubated at 37$^o$C for pre-set times. After incubation times, specimens were washed thoroughly with deionized (DI) water (more than 3 times) to remove any residual salt before freeze-drying, especially for the PBS degradation. Mass loss was calculated by Eq. (2). Here $W_0$ and $W_1$ are the initial weight and the weight after degradation respectively. Four (NaOH

degradation) or six (PBS degradation) specimens were averaged, and the results are presented as means ± standard deviation.

$$\text{Mass Loss (\%)} = \frac{W_0 - W_1}{W_0} \times 100\% \quad (2)$$

For *in vivo* degradation, disk–shaped specimens of POC; POC-click-1; POC-click-3, and PLLA samples (8 mm in diameter, with thickness around 0.75-0.95 mm) were implanted subcutaneously in the back of healthy, 3 month old, female Sprague Dawley (SD) rats (Harlan Sprague Dawley Inc., Indianapolis, IN) after being sterilized with 70% ethanol, sterilized PBS (pH 7.4), and UV light in sequence followed by drying in a cell culture hood overnight. Four specimens were used for each sample. After 20 weeks, the samples were harvested, washed thoroughly with PBS solution and DI water, and then freeze-dried. The mass loss was also calculated by Eq. (2). The results are shown in Figure 1.

***In Vitro* Cell Cytotoxicity Study**

The relative cytotoxicity of POC-click-1, POC-click-2, and POC-click-3 were assessed with a MTT (methylthiazolyldiphenyl-tetrazolium bromide) assay against NIH 3T3 fibroblasts. POC and PLLA were used as the positive and negative control, respectively. Samples were cut into discs (7 mm) to fit the inner diameter of 96-well plates. The samples were sterilized by treating with 70% ethanol, sterilized PBS (pH 7.4), and UV light in sequence. Subsequently, 200 μL of a cell suspension (density of $5\times10^4$ cells/mL) in Dulbecco's modified eagle's medium (DMEM, with 10% fetal bovine serum (FBS)) was added to each well in a 96-well plate with disk-shaped specimens on the bottom. Samples without cells were used as control. MTT assay

analysis was performed after incubating for 1, 3, and 7 days in an incubator (37 $^{o}$C, 5% $CO_2$) as described in previous work. [11] The result is shown in Figure S11.

**Foreign Body Response**

To assess the inflammatory response towards TSB cross-linked POC-click polymer films *in vivo*, POC-click-1 and POC-click-3 were chosen as the representatives of POC-click polymers to determine the foreign body response using H & E staining and CD11b staining. POC and PLLA films were used as positive and negative control, respectively. Disk-shaped films (8 mm in diameter, with thickness around 0.75-0.95 mm) were implanted subcutaneously in the upper or lower back of healthy 3 month old female Sprague Dawley (SD) rats (Harlan Sprague Dawley Inc., Indianapolis, IN) after being sterilized and dried in the cell-culture hood as described above. Nine SD rats were divided into 3 groups with 3 rats each for 3 different time points (1, 4 and 12 weeks) of the study. At the end of each time point, 3 rats were sacrificed with excess $CO_2$, and polymer films with surrounding tissues were harvested and fixed by soaking in 10% formalin for 2 days. The samples were processed on an automated tissue processor, embedded in paraffin wax, and sectioned into 4-μm sections. Six slides from different areas of the explants were stained with hematoxylin and eosin staining. [12] To characterize the presence of inflammatory cells, another 6 slides were stained with inflammatory cell marker CD11b (rat anti-mouse MAC-1, Santa Cruz Biotechnology) and peroxidase-conjuagated goat anti-rat secondary antibodies (Jackson ImmunoResearch Laboratories, PA). [13] Next, the CD11b staining slides were treated with 3, 3-diaminobenzidine substrate system and counterstained with

hematoxylin. The positive immunoreactions appeared as dark brown staining on a blue background. The cross-sections were examined using a Leica DMLP microscope (Leica Microsystems Inc., Bannockbum, IL) fitted with a Nikon E500 CCD camera (Nikon Corp., Japan). For quantitative analysis, all the cells in a 200 × 200 $\mu m^2$ region of the skin-side tissue near the implant films from 400× images of H & E staining were counted. For one sample, at least 8 different square regions from different specimens (implanted in different rats) were analyzed and the numbers were averaged. The CD11b+ cells (with dark brown staining on a blue background) from the 400× images were also counted using the same method. The results are shown in Figure S12.

**P15 Conjugation on POC-click-3 Film and Endothelial Cell (EC) Cell Attachment and Proliferation**

P15 was first modified by copper-free clickable moieties to obtain clickable p15. Briefly, p15 was reacted with click-easy ™ BCN N-hydroxysuccinimide ester I in DMSO solution at room temperature for 24 hrs to obtain clickable p15 (Scheme S1). A designated amount of DMSO solution of clickable p15 was diluted with DI water (v/v of water/DMSO = 1/1) and used directly for strain-promoted alkykyne-azide cycloaddition (SPAAC) with POC-click-3 films (37$^{o}$C, 3d). P15 conjugated POC-click-3 films were obtained after being washed with DI water followed by freeze-drying. The p15 conjugated POC-click-3 (POC-click-3-p15) film was characterized by FTIR and UV-vis spectra (using Weber's modified Sakaguchi reaction of guanidine group [14] on p15) (Figure S7). The amount of p15 conjugated

on the film was also determined by UV-vis spectra (each p15 molecule contains one guanidine group, the p15 standard curve after Sakaguchi reaction was shown in Figure S8) to be 10.6 nmol/cm$^2$, which is sufficient for endothelial cell attachment according to literature. [15]

POC-click-3-p15 along with pure POC-click-3 (100$^o$C, 3d, used as control) samples were die-cut into discs with a diameter of 7 mm that matches the inner diameter of 96-well plates. The samples were all sterilized by treating with 70% ethanol, sterilized PBS (pH 7.4), and UV light in sequence and incubated in Dulbecco's Modified Eagle's Medium (DMEM) at 37$^o$C for 3-7 days prior to cell seeding. Primary human umbilical vein endothelial cells (HUVECs) were cultured in Endothelial Cell Growth Medium Bulletkit from Lonza (EGM-2 BulletKit) according to the manufacturer's instructions. The EGM-2 BulletKit contains a 500 mL EBM-2 Basal Medium and a set of supplements, EGM-2 SingleQuot Kit Suppl. & Growth Factors. All supplements were added to the 500 ml of EBM-2 Basal Medium before use. Cells were incubated at 37$^o$C with 5% $CO_2$. The media was changed every other day. HUVEC cells were cultured until the third passage and seeded on the films in a 96-well plate (5000 cells/well) and incubated for 1, 3, and 7 days. Next, MTT reagent (5mg/mL, 20uL/well) was added to studied wells and the mixture was incubated at 37 °C for another 4 hours. The absorbance of the samples after MTT assay was measured via micro-plate reader at 570 nm. At the same time for each time point (day 1, 3 and 7), HUVECs on both p15 conjugated POC-click-3 samples and POC-click3 samples were stained by Live/Dead Viability/Cytotoxicity Kit (Invitrogen, molecular

probes, Eugene, OR) for the observation of cell morphology and spreading using an inverted light microscope (Nikon Eclipse Ti-U) equipped with a ANDOR DL-604M-#VP camera and Prior Lumen 200. In addition, the morphology and spreading of HUVEC on POC-click-3-p15 and POC-click-3 samples at day 7 was imaged by scanning electron microscopes (SEM, FEI, Quanta 200) after the cells were fixed with 2.5% (wt/v) glutaraldehyde-PBS solution, followed by sequential dehydration by treatment with a graded series of ethanol (50%, 75%, 95% and 100%) and freeze-drying. All the results are shown in Figure 2.

**Tubular Biphasic Scaffold (TBS) Preparation and p15 Conjugation**

Biphasic small diameter vascular graft scaffolds of POC-click-3, POC, and CUPE composed of a rough inner lumen surface, middle porous layer with pore size of 1-20 μm, and outer porous layer with pore size of 150-250 μm (see Figure 6) were fabricated as adapted from previous methods to replicate the stratified architecture of native blood vessels. [16, 17, 18] Briefly, steel rods with 3mm outer diameter were dip coated with a pre-polymer solution (30% w/w for POC and POC-click3, 3% w/w for CUPE) in 1, 4-dioxane, and coated with NaCl (99% purity) with an average size of 1-20 μm. Next, NaCl with a size of 1-20μm was mixed with a pre-polymer solution in a 1:5 polymer to salt weight ratio, and mixed until a viscous paste was formed. The paste was then transferred onto the steel rods to create a 200 μm thick layer. The entire construct was allowed to air dry and then crosslinked at 100$^{o}$C for 1 day. Next, another viscous pre-polymer-salt paste, made from a mixture NaCl (150-250μm) and pre-polymer solution in a 1:10 polymer to salt weight ratio, was transferred over the

previous layer to create an 800μm thick layer. The steel rod/material assemblies were placed in a laminar flow hood overnight to remove all the solvent, and then transferred to an oven maintained at 100°C for another 3 days for crosslinking. After crosslinking, salt leaching was conducted by immersing the rod/material assemblies in DI water with complete water changes every 6 hours. The complete removal of salt was determined by testing with silver nitrate. The scaffolds were de-molded by swelling in 50% (v/v) ethanol solution in water followed by freeze-drying. Scaffold morphology was examined by scanning electron microscopy (SEM) (Hitachi S-3000N, Hitachi Science System, Ibaaki, Japan).

The mechanical properties, including peak load, suture retention, and burst pressures of POC-click-3, POC and CUPE TBSs were measured according to literature methods. [17]

P15 conjugated POC-click-3 TBS was obtained by SPAAC between clickable p15 and the inside layer of POC-click3 TBS by adding clickable p15 solution in DMSO into the inside hole of the biphasic scaffold with one end clipped. After reacting at 37°C for 3 days, the scaffold was washed with DI water and then freeze-dried. So-obtained p15 conjugated POC-click-3 scaffold was characterized by FTIR as well as UV-vis spectrometer (to verify p15 conjugation by Weber's modified Sakaguchi reaction of guanidine group [14] on p15). The results are shown in Figure 2.

**Thermal properties and wettability results**

Thermal properties of POC film (100°C, 3d) and POC-click-x films (100°C, 3d) made by heating the equal-weight mixtures of pre-POC-$N_3$-x and pre-POC-Al-x (x =

1, 2, or 3), were characterized by differential scanning calorimetry (DSC) (Figure S13A) and thermal gravimetric analysis (TGA) (Figure S13B). DSC curves shown in Figure S5A indicated apparent glass transition temperatures ($T_g$) for all polymers. Increasing the amount of click moieties in the cross-linked polymer films resulted in the increase of $T_g$ due to the formation of rigid triazole rings by thermal click reactions, which also agrees with previous reports. [19-22] TGA curves (Figure S13B) showed that all polymers were relatively stable with their thermal decomposition temperatures ($T_d$) all higher than 218$^o$C. POC showed a second highest $T_d$ of 241.6$^o$C. POC-Al-3 had the highest $T_d$, and POC-$N_3$-3 had the lowest $T_d$, while the $T_d$s of the POC-click polymers fell in between.

The wettability of POC-click polymers assessed by water-in-air contact angle tests using POC and poly(L-lactic acid) (PLLA) as controls. As shown in Figure S10, POC-click-1 and POC-click-2 showed similar wettability to POC, especially after 30 minutes of water contact. Both were more hydrophilic than PLLA. Although the contact angle of POC-click-3 was even higher than that of PLLA in the beginning, it became much lower than that of PLLA after 30 minutes, indicating the hydrophilic nature of POC-click backbones.

**Results of *in vitro* and *in vivo* cytocompatibility of POC-click polymers**

The *in vitro* cytocompatibility of POC-click polymers was assessed by a methyl tetrazolium (MTT) assay against 3T3 fibroblastic cells using POC and PLLA as controls. The MTT result in figure S11 shows that all polymers supported 3T3 fibroblastic cell proliferation and displayed a similar growth pattern. The proliferation of 3T3 cells on POC-click polymers was also found to be better than on POC. The

MTT result suggested that the introduction of click moieties into polyester elastomers may improve the cytocompatibility of so-obtained polymers. It was reasoned that the introduction of triazole rings in POC polymers may counteract the acidity of POC polymers.

The *in vivo* cytocompatibility (foreign body response) of POC-click polymers was studied by a subcutaneous implantation of POC-click-1 and POC-click-3 films in SD rats, respectively, using POC and PLLA as controls. As shown in Figure S12, all samples implanted for 1 week produced a slight acute inflammatory response, which is a general process that is expected and consistent with the introduction of a foreign material into the body and can be confirmed by the cell infiltration (H & E staining, Figure S12A) as well as the appearance of CD11b positive cells (CD11b staining, Figure S12B) in the tissues surrounding the polymer films. Cell densities surrounding different polymer implants were not statistically different and declined over time (Figure S12C and S12D). After 12 weeks of implantation, most of the cells surrounding the samples were fibroblast cells (Figure S12A). CD11b positive cells were rarely seen after 12 weeks (Figure S12B and S12D), indicating that minor chronic inflammatory reaction took place. The mild inflammatory response suggested that POC-click polymers and their degradation products were as cytocompatible as the controls, POC and PLLA, further indicating the introduction of click moieties does not compromise the biocompatibility of the so-obtained polymers.

**Scheme S1.** P15 functionalization for strain-promoted alkykyne-azide cycloaddition (SPAAC).

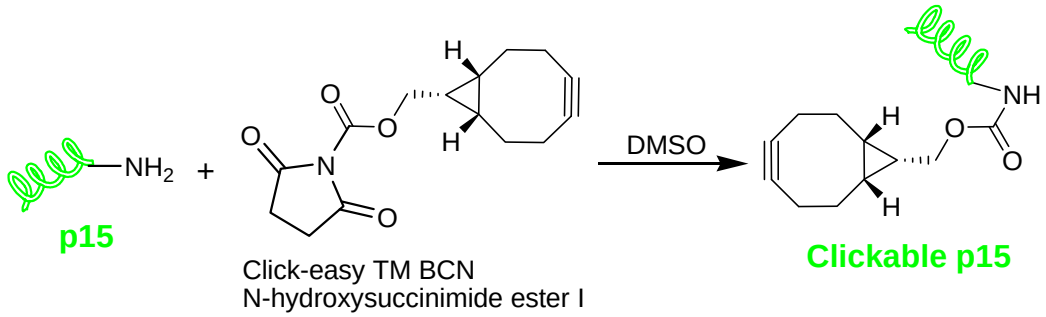

**Scheme S2**: The chemical structure of TSB cross-linked POC-click polymer.

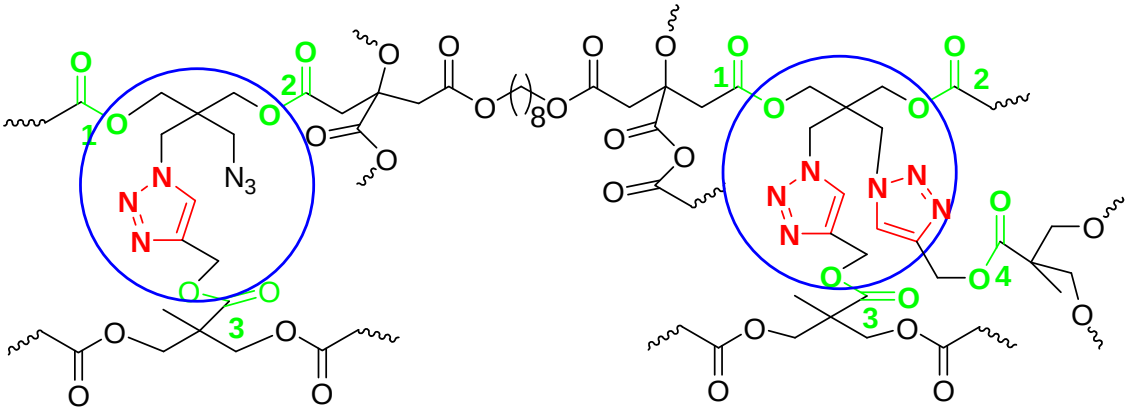

**Figure S1.** FTIR and $^{1}$H-NMR spectra of POC-$N_3$ pre-polymer series and POC pre-polymer.

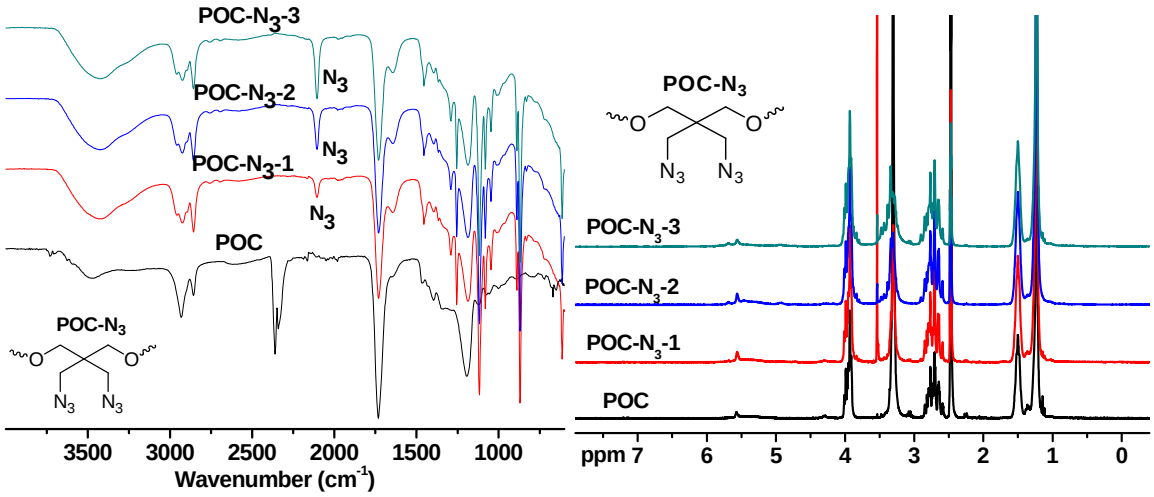

**Figure S2.** $^{1}$H-NMR and FTIR spectra of POC-Al pre-polymer series and POC pre-polymer.

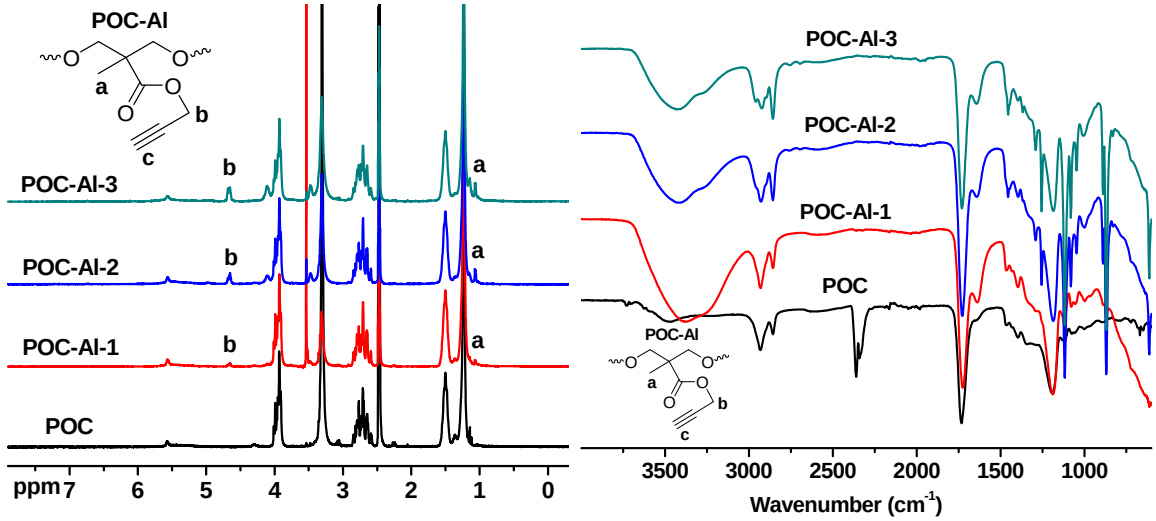

**Figure S3.** FTIR spectra of (**A**): POC-$N_3$-1 before and after heating at different temperatures for different times; (**B**): Equal-weight mixture of pre-POC-$N_3$-1 and pre-POC-Al-1 [POC-$N_3$-1, Al-1 (1/1)] before and after heating at different temperatures for different times.

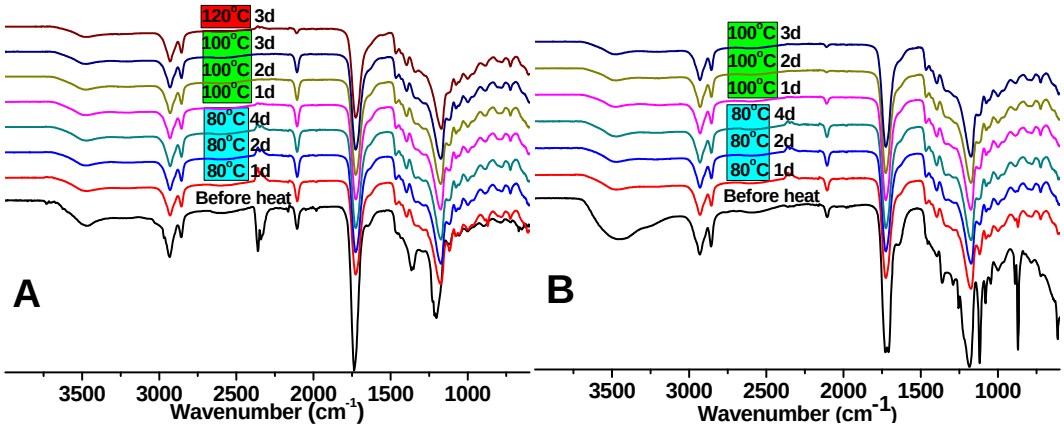

**Figure S4.** FTIR spectra of POC-click-x series films made from the mixture of pre-POC-$N_3$-x and pre-POC-Al-x (x = 1, 2 or 3, w/w = 1/1) after heating at 100 $^{o}$C for 3 days.

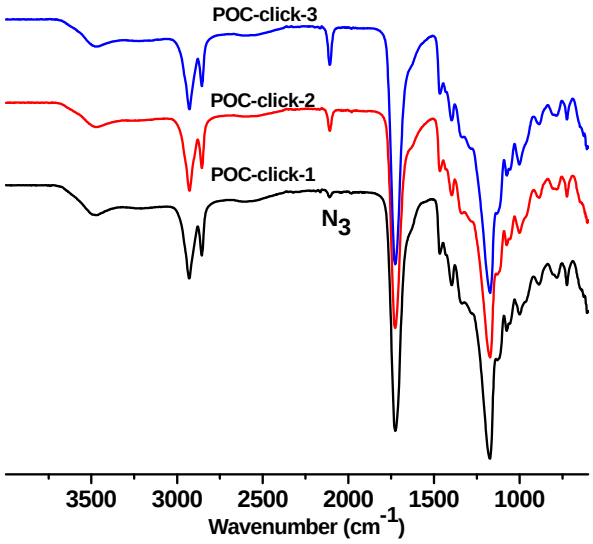

**Figure S5**. Mechanical properties of POC-click cross-linked polymer (100°C, 3d) series made from mixtures of POC-$N_3$-x and POC-Al-y (x, y=1, 2 or 3 and x ≠ y) with different weight ratios.

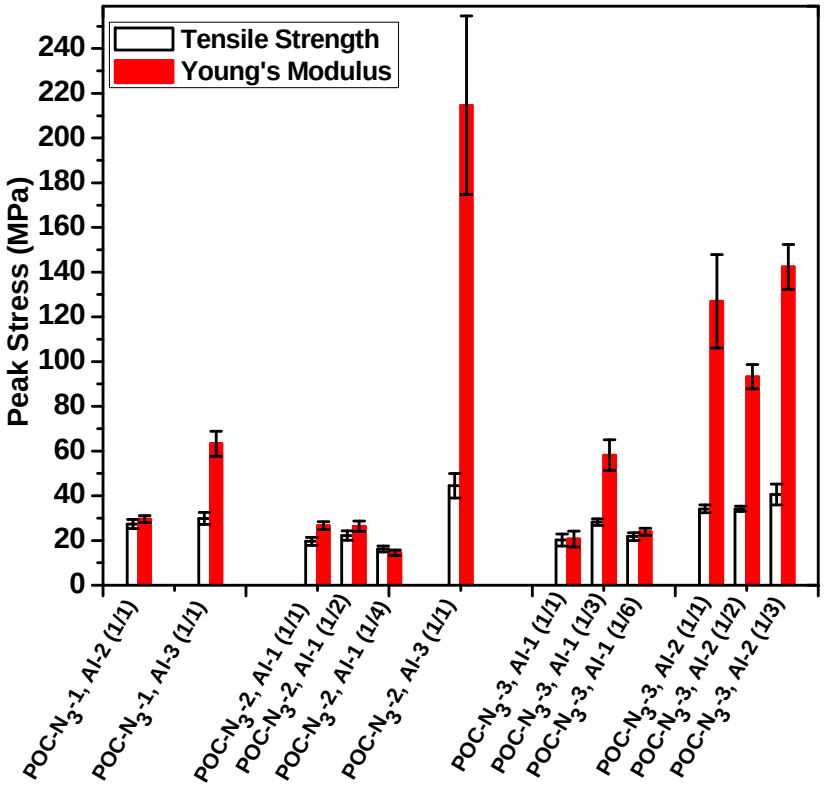

**Figure S6**. Mechanical properties of (A) cBPLP-ser, cBPLP-ser-$N_3$, cBPLP-ser-Al and cBPLP-click (cBPLP-Ser-$N_3$, Al) polymers, insert is the image of the films under UV light in dark; (B) CUPE, CUPE-$N_3$, CUPE-Al and CUPE-click (CUPE-$N_3$, Al) polymers. All the polymers were cross-linked at 100$^{o}$C for 3 days.

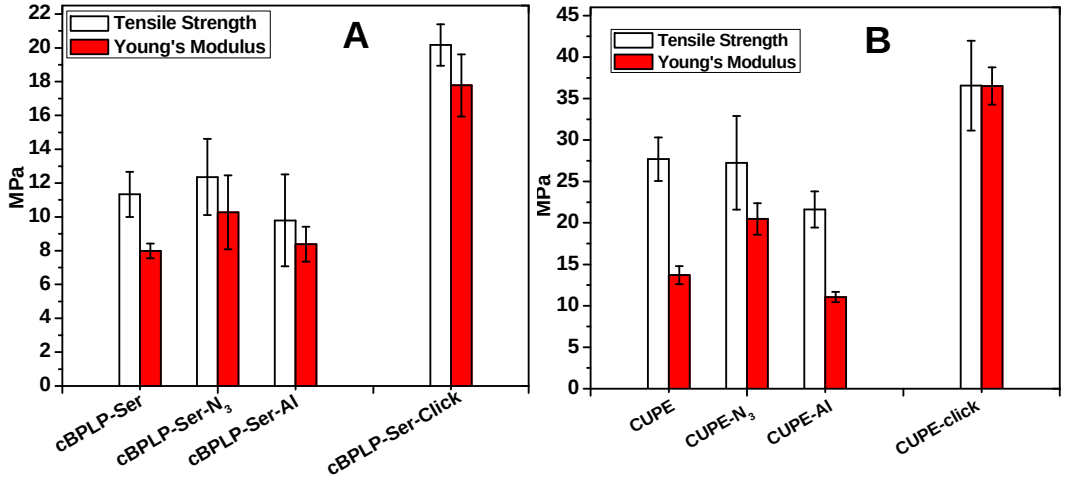

**Figure S7**. FTIR (A) and UV-vis (B, after Sakaguchi reaction of a 2 $cm^2$ film for each sample, the spectrums were recorded after the films were completely dissolved in the basic solution, using POC-click3 solution itself as base line) spectra of the POC-click-3 (POC-$N_3$-3, Al-3 (1/1)) film before and after p15 conjugation; C: Comparison of growth and proliferation of human umbilical vein endothelial cells (HUVECs) on p15 conjugated POC-click-3 (POC-click-3-p15) films and POC-click-3 films (used as control). MTT absorption was measured at 570 nm, N=8. ***p*<0.05 and #*p*>0.05.

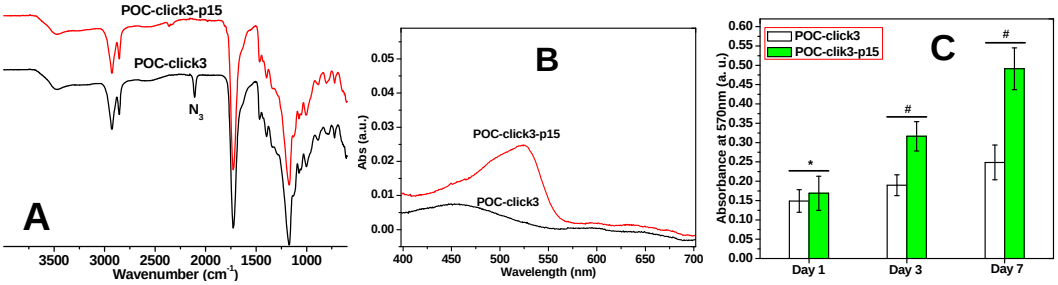

**Figure S8**. Standard curve of Sakaguchi reaction used to determine p15 (contains 1 guanidine group per molecule) concentration. Here p15 itself was used as the standard, absorbance at 525 nm exhibits a liner correlation to p15 concentration. Insert is the general UV-vis spectrum of p15 solution in DI water after Sakaguchi reaction (up left) and the liner formula and corresponding data of the fitted curve (down right).

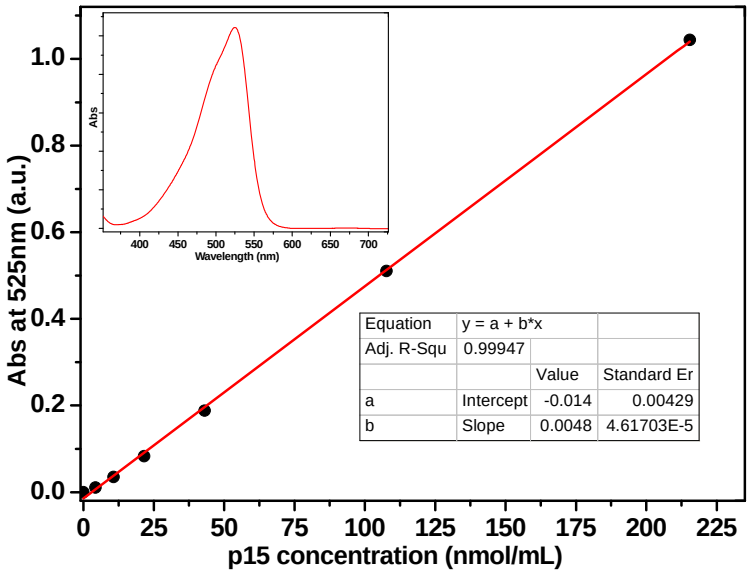

**Figure S9.** FTIR (A) spectra and UV-vis (B, after Sakaguchi reaction of a 1 cm length insider layer of the biphasic scaffold of each sample, the spectrums were recorded after the inside layer being totally dissolved in the basic media, using unmodified insider layer scaffold itself as base line) spectra of the inside layer of POC-click-3 biphasic scaffold before and after p15 conjugation.

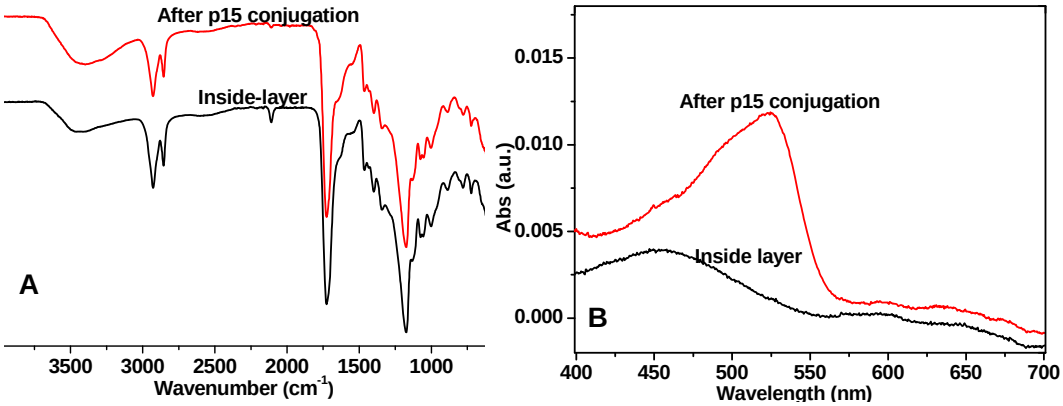

**Figure S10.** The water-in-air contact angle (θ) vs. time curves of dual cross-linked POC-click polymers (1000°C, 3d) series compared with controls (POC [100°C, 3d] and PLLA).

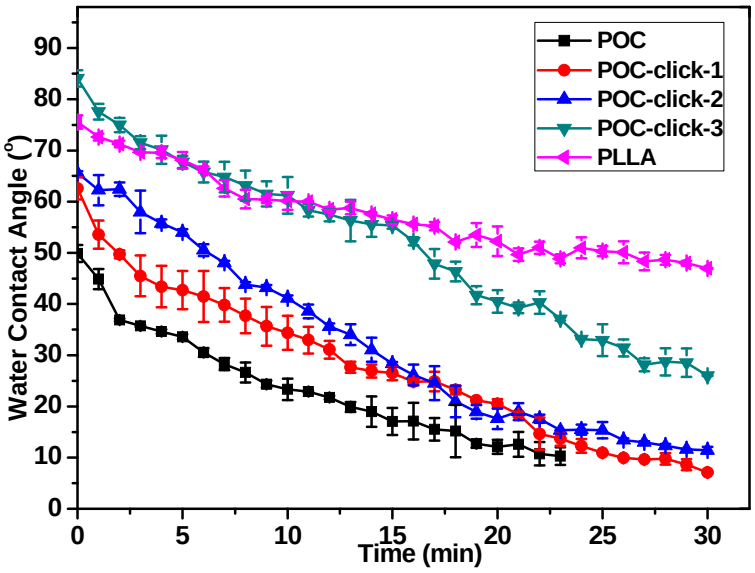

**Figure S11**: MTT assay against 3T3 fibroblast of cross-linked POC-click polymer films and controls (POC and PLLA). MTT absorption was measured at 570nm.

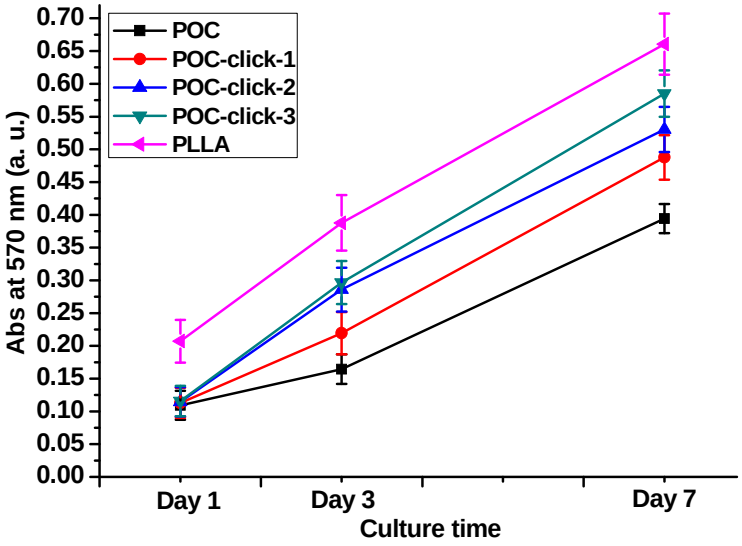

**Figure S12.** Foreign body response evaluations: Representative images of H & E (hematoxylin and eosin) (A) and immunohistochemical (for CD11b) (B) staining of sections of subcutaneously implanted polymer films (POC-click-1 and POC-click-3, using POC and PLLA as positive and negative control) with surrounding tissues (all skin-side regions), samples were harvested at 1 week, 4 weeks and 12 weeks following implantation; Averaged total (C) or CD 11b positive (D) cell numbers in a 200 × 200 $\mu m^2$ square region of the skin-side tissue near the implant films from 400× images of H & E staining (C) or CD 11b staining (D) with implantation times of 1, 4 and 12 weeks.

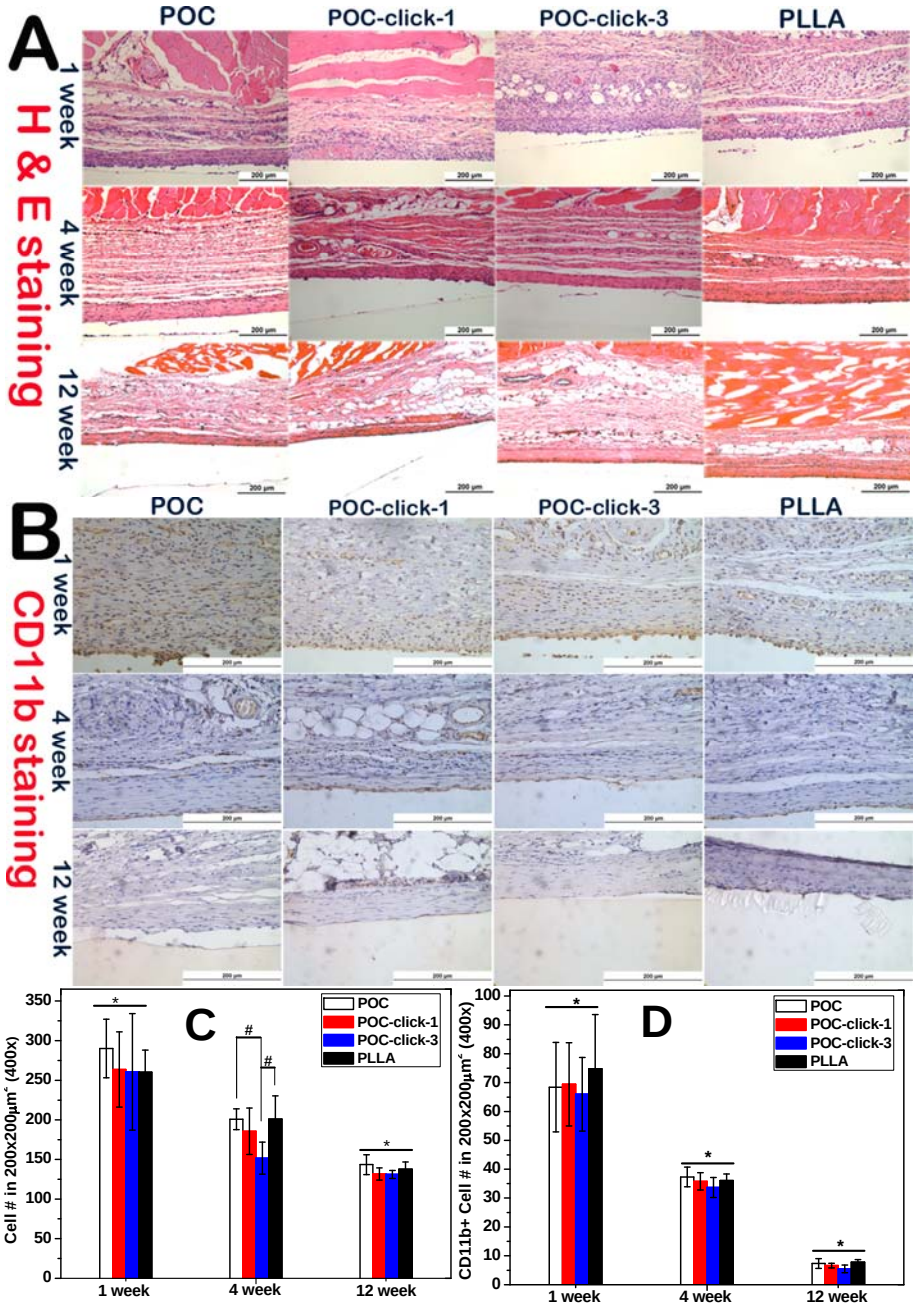

**Figure S13.** Thermal properties of POC-click film series and POC cross-linked film (100°C, 3d): (**A**) DSC curves; (**B**) TGA curves, the thermal decomposition temperatures ($T_d$) (5% decomposition) of the cross-linked polymer films are listed below: POC: 241.6 °C; POC-$N_3$-3: 218.2 °C; POC-Al-3: 248.9 °C; POC-click-1: 231.1 °C; POC-click-2: 230.2 °C; POC-click-3: 225.0 °C.

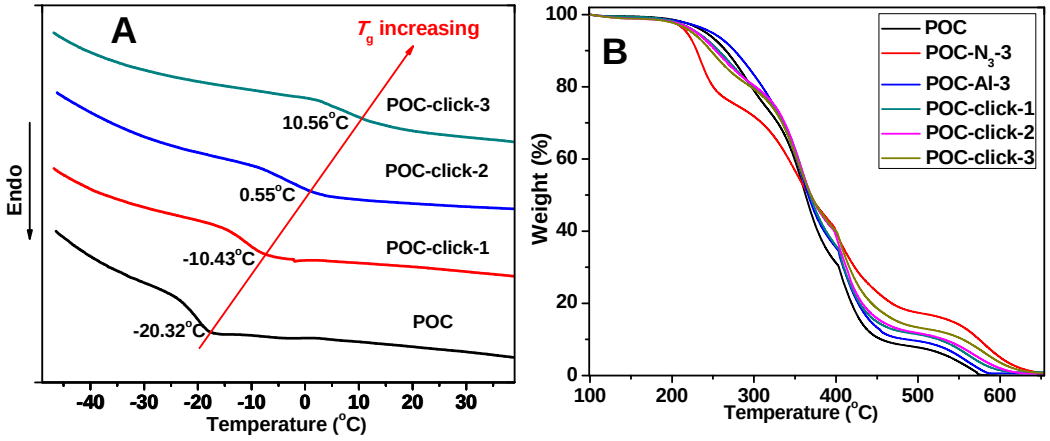

**Table S1**: Density measurements, mechanical tests and cross-linking characterization of POC, POC-click polymers, CUPE, cBPLP-Ser and their click versions. All cross-linked films were obtained by heating at 100°C for 3 days.

| Samples | Density (g/cm$^3$) | Tensile strength (MPa) | Young's modulus (MPa) | Elongation (%) | N (mol/m$^3$) | Mc (g/mol) |
|---|---|---|---|---|---|---|
| POC | 1.24±0.01 | 6.66±0.84 | 5.39±0.51 | 207.81±24.03 | 718±128 | 1763±331 |
| POC-click-1 | 1.24±0.04 | 18.30±3.95 | 16.61±1.29 | 323.88±52.59 | 587±34 | 2111±151 |
| POC-click-2 | 1.24±0.01 | 28.33±1.22 | 43.89±5.54 | 289.87±26.67 | 7225±911 | 173±22 |
| POC-click-3 | 1.27±0.01 | 41.32±2.67 | 275.93±49.71 | 77.99±25.43 | 34307±1995 | 35±6 |
| CUPE | 1.20±0.01 | 27.68±2.63 | 13.70±1.09 | 443.70±80.11 | 1902±143 | 631±53 |
| CUPE-click | 1.22±0.02 | 36.55±5.41 | 36.52±2.26 | 661.79±112.08 | 5003±351 | 244±19 |
| cBPLP-Ser | 1.22±0.01 | 11.33±1.33 | 7.99±0.44 | 274.22±44.16 | 1120±48 | 1093±42 |
| cBPLP-Ser-click | 1.23±0.02 | 20.17±1.23 | 17.78±1.83 | 241.42±13.67 | 2536±192 | 486±36 |

References


[1] X. Zhang, Z. Zhong, R. Zhuo, *Macromolecules* **2011**, *44*, 1755-1759.

[2] J. Xu, F. Prifti, J. Song, *Macromolecules* **2011**, *44*, 2660-2667.

[3] C. Lu, Q. Shi, X. Chen, T. Lu, Z. Xie, X. Hu, J. Ma, X. Jing, *J. Polym. Sci. Part A: Polym. Chem.* **2007**, *45*, 3204-3217.

[4] Q. Shi, X. Chen, T. Lu, X. Jing, *Biomaterials* **2008**, *29*, 1118-1126.

[5] J. Yang, A. R. Webb, G. A. Ameer, *Adv. Mater.* **2004**, *16*,511-516.

[6] J. Yang, A. R. Webb, S. J. Pickerill, G. Hageman, G. A. Ameer, *Biomaterials* **2006**, *27*, 1889-1898.

[7] J. Dey, H. Xu, J. Shen, P. Thevenot, S. R. Gondi, K. T. Nguyen, B. S. Sumerlin, L. Tang, J. Yang, *Biomaterials* **2008**, *29*, 4637-4649.

[8] J. Yang, Y. Zhang, S. Gautam, L. Liu, J. Dey, W. Chen, R. P. Mason, C. A. Serrano, K. A. Schug, L. Tang, *Proc. Natl. Acad. USA* **2009**, *106*, 10086-10091.

[9] Y. Wang, G. A. Ameer, B. Sheppard, R. Langer, *Nat. Biotechnol.* **2002**, *20*, 567-591.

[10] J. Yang, J. Bai, S. Wang, *Biomaterials* **2002**, *23*, 2607-2614.

[11] R. T. Tran, P. Thevenot, D. Gyawali, J.-C. Chiao, L. Tang, J. Yang, *Soft Matter* **2010**, *6*, 2449-2461.

[12] D. Gyawali, P. Nair, Y. Zhang, R. T. Tran, C. Zhang, M. Samchukov, M. Makarov, H. K. W. Kim, J. Yang, *Biomaterials* **2010**, *31*, 9092-9105.

[13] J. Zhou, Y.-T. Tsai, H. Weng, D. W. Baker, L. Tang, *Biomaterials* **2011**, *32*, 9383-9390.

14] Z. Zhang, Y. Lai, L. Yu, j. Ding, *Biomaterials* **2010**, *31*, 7873-7882.

[15] C. Li, A. Hill, M. Imran, *J. Biomater. Sci. Polymer Ed.* **2005**, *16*, 875-891.

[16] J. Yang, D. Motlagh, A. R. Webb, C. A. Ameer, *Tissue Eng.* **2005**, *11*, 1876-1886.

[17] J. Dey, H. Xu, K. T. Nguyen, J. Yang, *J. Biomed. Mater. Res. A*, **2010**, *95A*, 361-370.

[18] Y. Zhang, R. T. Tran, I. S. Qattan, Y.-T. Tsai, L. Tang, C. Liu, J. Yang, *Biomaterials* **2013**, *34*, 4048-4056.

[19] J. Guo, F. Meng, X. Li, M. Wang, Y. Wu, X. Jing, Y. Huang, *Macromol. Biosci.* **2012,** *12*, 533-546.

[20] J. Hong, Q. Luo, X. Wan, Z. S. Petrović, B. K. Shah, *Biomacromolecules* **2011,** *13*, 261-266.

[21] D. J. V. C. van Steenis, O. R. P. David, G. P. F. van Strijdonck, J. H. van Maarseveen, J. N. H. Reek, *Chem. Commun.* **2005,** 4333-4335.

[22] J. Guo, Y. Wei, D. Zhou, P. Cai, X. Jing, X.-S. Chen, Y. Huang, *Biomacromolecules* **2011,** *12*, 737-746.